

Numerical Simulation of Heat Source Property of Tube Cathode Arc and Influence on Weld Penetration Geometry in Anode Material

S. Tashiro, K. Yamamoto and M. Tanaka

Joining and Welding Research Institute, Osaka University, 11-1 Mihogaoka, Ibaraki, Osaka 576-0047

e-mail: tashiro@jwri.osaka-u.ac.jp

Tungsten Inert Gas (TIG) arc is the most widely employed type of a plasma torch and enables to produce arc plasma with high energy density. Therefore it is suitable as a heat source device especially for processes to require concentrating the heat input at a point. On the other hand, Tube Cathode Arc (TCA) to be a kind of TIG produces the arc plasma by introducing inner shielding gas through the central hole of the tube cathode. As the basic heat source property of argon (Ar) TCA, the property of the arc plasma and the heat input intensity onto a water-cooled copper anode for various inner shielding gas flow rates were numerically analyzed. Furthermore, by employing stainless steel SUS304 anode, the geometry of its weld penetration was also predicted. The results were compared with those for the conventional TIG. As a result, it was shown that since TCA enables to heat the target material uniformly by controlling the inner shielding gas flow rate and preserve it from damage due to excessive heat input during the process, it is suitable for processes such as brazing, buildup or thermal spraying.

Key words: Numerical simulation, Heat source property, Tube Cathode Arc, Weld penetration geometry

1. INTRODUCTION

Since a plasma torch can stabilize high temperature arc plasma by employing shielding gas, it is suitable as a heat source device. Tungsten Inert Gas (TIG) is the most widely employed type of the plasma torch and produces the arc plasma between a tungsten cathode and an anode material. It has high heating efficiency and highly controllable characteristics, and requires low cost for equipment investment. Furthermore, the target material can be heated without any chemical reaction by using inert gas as the shielding gas. Therefore, it is widely utilized, for example, for nano-particle production, material processing such as melting, cutting and welding [1], or decomposition, volume reduction and detoxification of toxic waste [2] and so on.

The heat source property of TIG strongly depends on the physical property of the shielding gas. For instance, helium gas with low electrical conductivity or carbon dioxide with high specific heat causes constriction of the arc plasma and, hence, enables to produce the arc plasma with high energy density [3]. Therefore, TIG is suitable especially for processes to require concentrating the heat input at a point but less effective for processes to require heating the target material uniformly.

On the other hand, Hollow Cathode Arc (HCA) to be a kind of TIG produces the arc plasma by introducing the shielding gas through a central hole of the hollow cathode. It has been studied as a heat source device especially in lower pressure, for example, for space welding [4] or plasma CVD [5], because it is suitable to supply the shielding gas in the electrode gap. Furthermore, as applications at the atmospheric pressure, it may be utilized for brazing, buildup or thermal spraying. In this case, it is expected that the anode material can be preserved from damage due to excessive heat input during the process, because heat input may

not be concentrated at a point in contrast to the TIG[6]. However, the heat source properties of HCA at the atmospheric pressure are not fully understood.

We terms HCA at the atmospheric pressure as Tube Cathode Arc (TCA), because the mechanism of electron emission is different from that in low pressure. In this paper, as the basic heat source property of argon (Ar) TCA, the property of the arc plasma and the heat input intensity onto a water-cooled copper anode for various shielding gas flow rates are numerically analyzed. Furthermore, by employing stainless steel SUS304 anode, the geometry of its weld penetration is also predicted. The results are compared with those for the conventional TIG.

2. SIMULATION MODEL

A tungsten cathode, arc plasma and an anode are described in a frame of cylindrical coordinate with axial symmetry around the arc axis. A calculation domain and details of the cathodes for TIG and TCA are shown in Figure 1. The outer diameter and the inner diameter only for TCA are 3.2mm and 1.6mm, correspondingly. The anode is a water-cooled copper or a stainless steel SUS304 for which temperature coefficient of surface tension above the melting point is given in Ref. [7]. The electrode gap is set to be 5mm. The arc current is set to be 200A. Ar is introduced at the flow rate of 10L/min. from outside of the cathode on the upper boundary. Only for TCA, that at the flow rate of 0.5 or 2.0L/min. is additionally introduced through the central hole of the tube cathode. It is defined as an inner shielding gas. The flow is assumed to be laminar. The arc plasma is assumed to be under the local thermodynamic equilibrium (LTE). Figure 2 shows photographs of TIG and TCA in case of 200A. Azimuthally uniform

expansion of the cathode spot can be confirmed also in case of TCA under this arc current range. The other numerical modeling methods are given in detail in our previous papers [8, 9]. The differential equations (1)-(6) are solved iteratively by the SIMPLEC numerical procedure [10]:

Mass continuity equation;

$$\frac{1}{r} \frac{\partial}{\partial r} (r \rho v_r) + \frac{\partial}{\partial z} (\rho v_z) = 0 \quad (1)$$

Radial momentum conservation equation;

$$\frac{1}{r} \frac{\partial}{\partial r} (r \rho v_r^2) + \frac{\partial}{\partial z} (\rho v_r v_z) = -\frac{\partial P}{\partial r} - j_z B_\theta + \frac{1}{r} \frac{\partial}{\partial r} \left(2r\eta \frac{\partial v_r}{\partial r} \right) + \frac{\partial}{\partial z} \left(\eta \frac{\partial v_r}{\partial z} + \eta \frac{\partial v_z}{\partial r} \right) - 2\eta \frac{v_r}{r^2} \quad (2)$$

Axial momentum conservation equation;

$$\frac{1}{r} \frac{\partial}{\partial r} (r \rho v_r v_z) + \frac{\partial}{\partial z} (\rho v_z^2) = -\frac{\partial P}{\partial z} + j_r B_\theta + \frac{\partial}{\partial z} \left(2\eta \frac{\partial v_z}{\partial z} \right) + \frac{1}{r} \frac{\partial}{\partial r} \left(r\eta \frac{\partial v_r}{\partial z} + r\eta \frac{\partial v_z}{\partial r} \right) \quad (3)$$

Energy conservation equation;

$$\frac{1}{r} \frac{\partial}{\partial r} (r \rho v_r h) + \frac{\partial}{\partial z} (\rho v_z h) = \frac{1}{r} \frac{\partial}{\partial r} \left(\frac{r\kappa}{c_p} \frac{\partial h}{\partial r} \right) + \frac{\partial}{\partial z} \left(\frac{\kappa}{c_p} \frac{\partial h}{\partial z} \right) + j_r E_r + j_z E_z - R \quad (4)$$

Current continuity equation;

$$\frac{1}{r} \frac{\partial}{\partial r} (r j_r) + \frac{\partial}{\partial z} (j_z) = 0 \quad (5)$$

Ohm's law;

$$j_r = -\sigma E_r, j_z = -\sigma E_z \quad (6)$$

where t is time, h is enthalpy, P is pressure, v_z and v_r are the axial and radial velocities, j_z and j_r are the axial and radial component of the current density, g is the acceleration due to gravity, κ is the thermal conductivity, C_p is the specific heat, ρ is the density, η is the viscosity, σ is the electrical conductivity, R is the radiation emission coefficient, E_r and E_z are the radial and axial components of the electric field defined by $E_r = -\partial V / \partial r$ and $E_z = -\partial V / \partial z$, respectively, where V is electric potential. The azimuthal magnetic field B_θ induced by the arc current is evaluated by Maxwell's equation.

$$\frac{1}{r} \frac{\partial}{\partial r} (r B_\theta) = \mu_0 j_z \quad (7)$$

where μ_0 is the permeability of free space.

In the solution of equations (1)-(6), special account needs to be taken at the electrode surface for effects of energy that only occur at the surface. At the cathode surface, additional energy flux terms need to be included in equation (4) for thermionic cooling due to the emission of electrons, ion heating, and radiation cooling. The additional energy flux for the cathode H_K is:

$$H_K = -\varepsilon \alpha T^4 - |j_e| \phi_K + |j_i| V_i \quad (8)$$

where ε is the surface emissivity, α is the Stefan-Boltzmann constant, ϕ_K is the work function of the tungsten cathode, V_i is the ionization potential of argon, j_e is the electron current density, and j_i is the ion current density. At the cathode surface, for thermionic emission of electrons, j_e cannot exceed the Richardson current density J_R [11] given by:

$$|j_R| = AT^2 \exp\left(-\frac{e\phi_e}{k_B T}\right) \quad (9)$$

where A is the thermionic emission constant for the cathode surface, ϕ_e is the effective work function for thermionic emission of the electrode surface at the local surface temperature, and k_B is the Boltzmann's constant. The ion-current density j_i is then assumed to be $|j_i| = |j_R|$ if $|j_i|$ is greater than $|j_R|$; where $|i| = |i_r| + |i_z|$ is the total current density.

At the anode surface, the energy flux is given by $H_A = -\varepsilon \alpha T^4 + |j| \phi_A$ (10), where ϕ_A is the work function of the anode material.

The simulation domain is shown in Fig. 1. The cathode is a tungsten rod of diameter 1.6 mm and length 30 mm. The anode is a copper rod of diameter 2.0 mm and length 30 mm. The arc plasma is shown between the cathode and the anode. The simulation domain is defined by the axial distance z and the radial distance r .

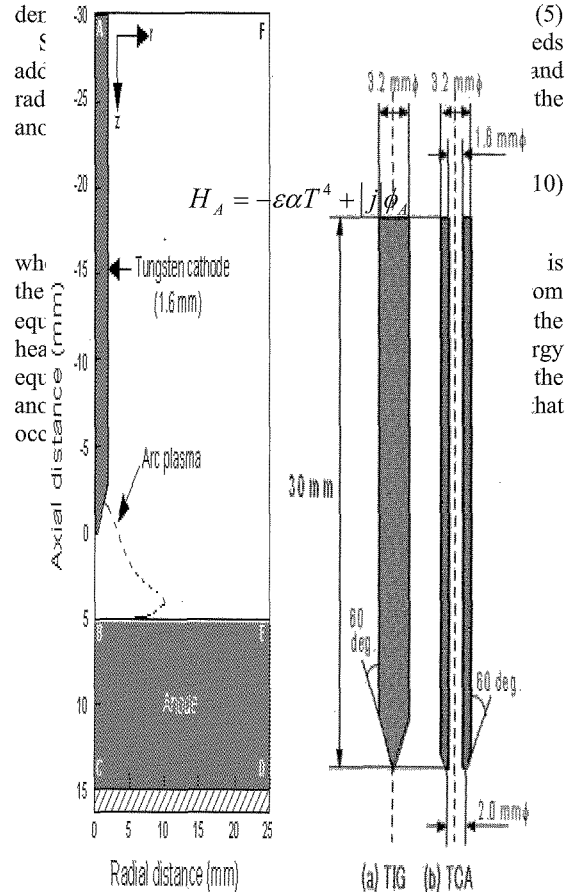


Fig. 1. Schematic illustration of simulation domain.

3. RESULTS AND DISCUSSION

Figure 3 shows Two-dimensional distribution of temperature and fluid flow velocity for TIG and TCA in the case of the water-cooled copper anode. Figure 4, 5 and 6 show radial distributions of the heat input intensity, current density and the arc pressure on the anode surface, respectively.

In the case of TIG, the current density near the arc axis becomes higher, since the arc current channel on the cathode tip is constricted at a point. The enhanced electromagnetic pinch force accelerates cathode jet velocity up to 320m/s and, thus, leads to high arc pressure to the anode surface. The increase in Joule heating due to the high current density lifts the plasma temperature near the cathode up to 21000K and cathode tip temperature up to 3500K near the melting point of tungsten. On the other hand, the heat input onto the anode surface is concentrated near the arc axis especially due to the concentration of the thermionic heating which is proportional to the current density. Consequently, the max. heat input intensity and the max. anode surface temperature reach 7000W/cm² and 750K, respectively.

Now, turn to the results for TCA. The current density decreases especially near the cathode due to the expansion of the arc current channel caused by the larger cathode tip area. It leads to the cathode jet velocity of approximately 70m/s which is 20% of the TIG and, thus, lower arc pressure especially in the case of low inner shielding gas flow rate. The plasma temperature and the cathode tip temperature reach only 13000K and 2900K which are 60% and 80% of the TIG because of the low current density. So, longer lifetime of the cathode can be expected. It is also seen that the plasma near the arc axis tends to be cooled by the inner shielding gas especially near the cathode and the low temperature region extends toward the anode with the increase of inner shielding gas flow rate. The max. heat input intensity onto the anode surface becomes less than 50% of the TIG. Additionally, the heat input intensity lowers near the arc axis for the higher inner shielding gas flow rate due to the low plasma temperature near the anode. And, the raise in the anode temperature decreases and becomes more uniform than the TIG.

Figure 7 shows Two-dimensional distribution of temperature and fluid flow velocity at 5 sec. after arc ignition for TIG and TCA in the case of stainless steel SUS304 anode. It can be seen that the radius and the depth of the weld penetration region in the anode reach 6.5mm and 1.3mm, respectively, in the case of TIG. On the other hand, in the case of TCA, the radius reaches 6.0mm which is approximately same as the TIG and, in contrast, the depth decreases with increase of the inner shielding gas flow rate to 0.5mm for 2L/min. It is recognized that an electromagnetic force strongly affects downward convective flow in the weld penetration region in the anode material [7]. In the case of TCA, it is considered that the weak electromagnetic force due to the low current density leads to the shallow weld penetration in addition to the effect due to the low max. heat input intensity. Consequently, it was found that TCA is suitable for processes such as brazing, buildup or thermal spraying because the anode material can be preserved from damage due to excessive heat input during the process.

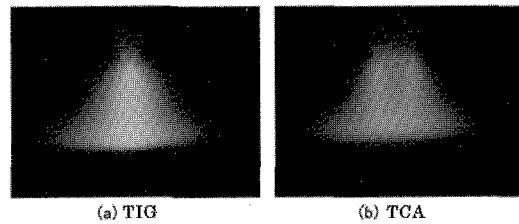


Fig. 2. Photographs of (a) TIG and (b) TCA.

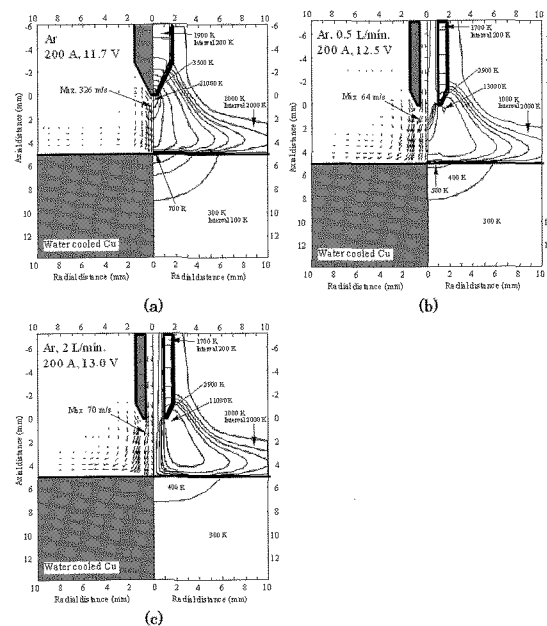


Fig. 3. Two-dimensional distribution of temperature and fluid flow velocity for (a) TIG, TCA at inner shielding gas flow rate of (b) 0.5L/min and (c) 2.0L/min in the case of water-cooled copper anode

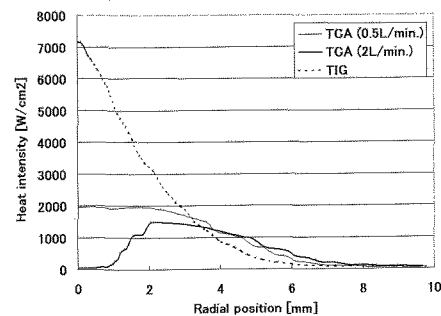


Fig. 4. Radial distributions of heat input intensity on the anode surface in the case of water-cooled copper anode

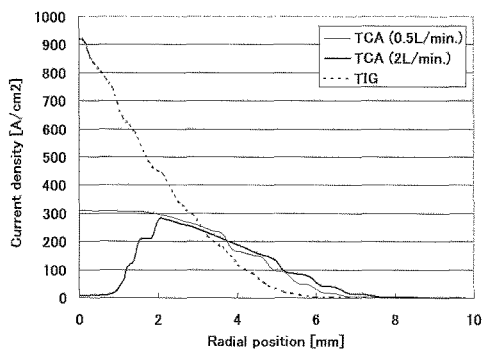


Fig. 5. Radial distributions of current density on the anode surface in the case of water-cooled copper anode

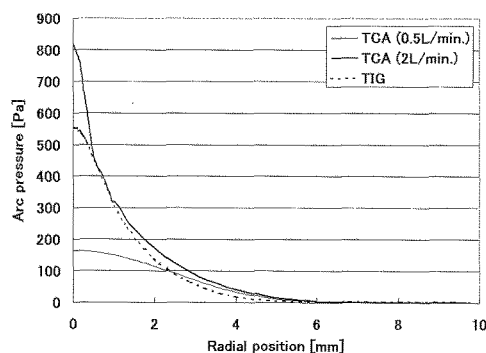


Fig. 6 Radial distributions of arc pressure on the anode surface in the case of water-cooled copper anode

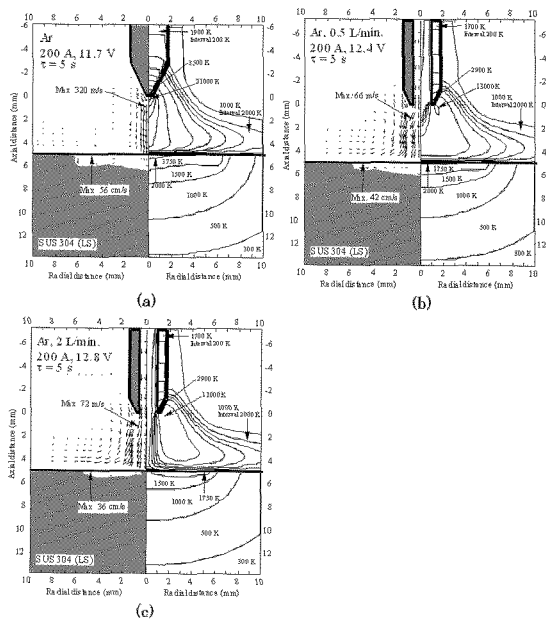


Fig. 7. Two-dimensional distribution of temperature and fluid flow velocity at 5 sec. after arc ignition for (a) TIG, TCA at inner shielding gas flow rate of (b) 0.5L/min and (c) 2.0L/min in the case of stainless steel SUS304 anode

4. CONCLUSIONS

The basic heat source property of argon TCA at the atmospheric pressure in 200A arc current for various inner shielding gas flow rates was numerically analyzed. Furthermore, the results were compared with those for the conventional TIG. The main conclusions are summarized as follows:

- 1) The current density for TCA decreases especially near the cathode than the TIG due to the expansion of the arc current channel caused by the large cathode tip area. It leads to the max. plasma temperature of 13000K and the cathode jet velocity of 70m/s which are 60% and 20% of the TIG, respectively.
- 2) The cathode tip temperature reaches only 2900K which is 80% of the TIG because of the low current density. So, longer lifetime of the cathode can be expected.
- 3) The max. heat input intensity onto the anode surface becomes less than 50% of the TIG because of the lower current density. Furthermore, it lowers also for the higher inner shielding gas flow rate. As a result, the raise in the anode temperature becomes lower and more uniform than the TIG.
- 4) The radius of the weld penetration region in the stainless steel SUS304 anode reach 6.0mm which is approximately same as the TIG and, in contrast, the depth decreases with increase of the inner shielding gas flow rate to 0.5mm for 2L/min. As a result, it was found that TCA is suitable for processes such as brazing, buildup or thermal spraying, because the anode material can be preserved from damage due to excessive heat input during the process.

References

- [1] M. Ushio M et. al., *IEEE Trans P. S.* **32**, 108 (2004).
- [2] T. Inaba et. al., *IEEE Trans D. E. I.* **7**, 684 (2000).
- [3] M. Tanaka et. al., *Vacuum* **73**, 381 (2004).
- [4] Y. Suita et. al., *Welding Int* **8**, 269 (1994).
- [5] G. F. Zhang et. al., *Diamond related materials* **8**, 2148 (1999).
- [6] T. Tamaki et.al., *Trans. MRS-J*, **32**, 539 (2007).
- [7] T. Zacharia et. al., *Metall Trans B* **21**, 600 (1990).
- [8] M. Tanaka et. al., *Metal Trans A* **33**, 2043 (2002).
- [9] M. Tanaka, et.al., *Plasma Chem. Plasma Process*, **23**, 585 (2003).
- [10] S. V. Patanker, "Numerical heat transfer and fluid flow" Washington DC, Hemisphere Publishing Corporation, 1980
- [11] E. Pfender, "Electric Arcs and Arc Gas heaters, Ch. 6", published in M. H. Hirsh and H. J. Oskam, *Gaseous Electronics*, Academic Press, NewYork (1978) 291.

(Received December 14, 2007 ; Accepted February 5, 2008)